AIP Journal of Applied Physics

The electronic band structure of GaBiAs/GaAs layers: Influence of strain and band anti-crossing

Z. Batool, K. Hild, T. J. C. Hosea, X. Lu, T. Tiedje, and S. J. Sweeney

Citation: Journal of Applied Physics **111**, 113108 (2012); doi: 10.1063/1.4728028
View online: http://dx.doi.org/10.1063/1.4728028
View Table of Contents: http://scitation.aip.org/content/aip/journal/jap/111/11?ver=pdfcov
Published by the AIP Publishing

The electronic band structure of GaBiAs/GaAs layers: Influence of strain and band anti-crossing

Z. Batool,[1] K. Hild,[1] T. J. C. Hosea,[1,2,a)] X. Lu,[3,4] T. Tiedje,[5] and S. J. Sweeney[1,b)]
[1]*Advanced Technology Institute and Department of Physics, University of Surrey, Guildford, Surrey GU2 7XH, United Kingdom*
[2]*Ibnu Sina Institute for Fundamental Science Studies, Universiti Teknologi Malaysia, Johor Bahru, Johor 81310, Malaysia*
[3]*Department of Physics and Astronomy, University of British Columbia, Vancouver, V6T 1Z4, Canada*
[4]*Varian Semiconductor Equipment Associates, Gloucester, Massachusetts 01930, USA*
[5]*Department of Electrical and Computer Engineering, University of Victoria, Victoria BC, V8W 3P6, Canada*

(Received 3 April 2012; accepted 3 May 2012; published online 13 June 2012)

The $GaBi_xAs_{1-x}$ bismide III-V semiconductor system remains a relatively underexplored alloy particularly with regards to its detailed electronic band structure. Of particular importance to understanding the physics of this system is how the bandgap energy E_g and spin-orbit splitting energy Δ_o vary relative to one another as a function of Bi content, since in this alloy it becomes possible for Δ_o to exceed E_g for higher Bi fractions, which occurrence would have important implications for minimising non-radiative Auger recombination losses in such structures. However, this situation had not so far been realised in this system. Here, we study a set of epitaxial layers of $GaBi_xAs_{1-x}$ ($2.3\% \leq x \leq 10.4\%$), of thickness 30–40 nm, grown compressively strained onto GaAs (100) substrates. Using room temperature photomodulated reflectance, we observe a reduction in E_g, together with an increase in Δ_o, with increasing Bi content. In these strained samples, it is found that the transition energy between the conduction and heavy-hole valence band edges is equal with that between the heavy-hole and spin-orbit split-off valence band edges at $\sim 9.0 \pm 0.2\%$ Bi. Furthermore, we observe that the strained valence band heavy-hole/light-hole splitting increases with Bi fraction at a rate of ~ 15 (± 1) meV/Bi%, from which we are able to deduce the shear deformation potential. By application of an iterative strain theory, we decouple the strain effects from our experimental measurements and deduce E_g and Δ_o of free standing GaBiAs; we find that Δ_o indeed does come into resonance with E_g at $\sim 10.5 \pm 0.2\%$ Bi. We also conclude that the conduction/valence band alignment of dilute-Bi GaBiAs on GaAs is most likely to be type-I. © *2012 American Institute of Physics*. [http://dx.doi.org/10.1063/1.4728028]

I. INTRODUCTION

The bismide alloy $GaBi_xAs_{1-x}$ has attracted much attention due to its interesting band structure. The replacement of a small percentage of arsenic by bismuth in GaAs produces a giant reduction in the bandgap energy (E_g) of 60–90 meV/%Bi.[1–3] This has been described using a valence band (VB) anti-crossing interaction between the Bi level and the host GaAs VB (Ref. 3) analogous to conduction band (CB) anti-crossing now widely reported for dilute nitride alloys.[4] As the result of this anti-crossing, the VBs split into six valence sub-bands, which may be grouped into the $E_+(HH^+, LH^+, SO^+)$ and $E_-(HH^-, LH^-, SO^-)$ levels, where HH and LH refer to heavy and light holes, respectively, and SO to the spin-orbit split off band.[3] As bismuth is the heaviest non-radioactive group V element, its alloying to GaAs enhances the SO splitting energy (Δ_o), and thus, it is also interesting in the field of spintronics.[5] Furthermore, if Δ_o can be made to be larger than E_g, the valence band Auger process (conduction, heavy hole)-(split-off hole, heavy hole) ("CHSH") (Ref. 6) may be suppressed in the near-infrared wavelength region. Tailoring both E_g and Δ_o could make bismides potentially useful, e.g., for improved operating efficiency of 1.3–1.6 μm laser diodes, optical amplifiers, and optical modulators important for optical fibre communications.[7,8] A thorough understanding of the fundamental physical properties of bismides is therefore crucial. Whilst there are several reports in the past decade on the structural, optical,[1–3,5] thermal,[9–11] and transport properties[12] of bismides, they remain a relatively underexplored family of alloys.

Here, we present the results of comprehensive optical studies of $GaBi_xAs_{1-x}$ with bismuth concentrations of up to $x = 10.4\%$ grown compressively strained on a GaAs substrate. Optical absorption measurements of the fundamental bandgap energy in $GaBi_xAs_{1-x}$ with similar high Bi concentrations have been reported,[13] but the spin-orbit splitting energy Δ_o has not been measured beyond a concentration of $x = 8.4\%$.[3] Here, in addition to a bowing of the band-gap and spin-orbit splitting energies, we observe a cross over in energy between the CB-to-HH^+ transition and the HH^+-to-SO^+ transition. We also report for the first time the shear deformation potential (b) for this alloy calculated from the valence band heavy-hole/light-hole (HH^+-LH^+) splitting. By application of a novel iterative strain calculation, we are able to deduce the spin-orbit splitting energy and fundamental

a)E-mail: J.Hosea@surrey.ac.uk.
b)E-mail: S.Sweeney@surrey.ac.uk.

bandgap energy in unstrained analogues of our samples and report the bismuth concentration at which these two energies become equal, of importance to device applications. Finally, we comment on the likely conduction/valence band alignment configuration of GaBiAs grown on GaAs.

The investigated samples are $GaBi_xAs_{1-x}$ epilayers, grown on undoped (100) GaAs by molecular beam epitaxy with bismuth concentrations of $x = 2.3\%$, 4.5%, 8.5%, and 10.4%. The samples are all uncapped with the exception of the 2.3% sample, which is capped with 300 nm of GaAs. Further details about growth can be found in Ref. 14. The thicknesses of GaBiAs layers (30–40 nm) are all below the estimated critical thicknesses[1] and so are fully strained (pseudomorphic) to the GaAs substrate, as confirmed by earlier x-ray diffraction (XRD) studies of Bi concentrations up to 10%.[1,14] As evidence for this, Fig. 1 shows the XRD reciprocal space map of the substrate and GaBiAs film peaks for the highest concentration studied here of $Bi = 10.4\%$. This demonstrates that the GaBiAs film has the same in-plane lattice constant as the GaAs substrate, to within the measurement error of better than $\pm 2\%$.

In order to study the band structure of this material, we used photomodulated reflectance (PR) spectroscopy, which is considered to be an excellent technique due to its sensitivity to critical point transitions in the band structure.[15] In this contactless and non-destructive form of modulated reflectance spectroscopy, the material dielectric function is periodically perturbed by a chopped laser beam. When the laser is on, it generates electron-hole pairs, which drift apart under the influence of the in-built electric field and are captured by traps reducing the magnitude of the field. When the laser is off, the traps depopulate and the field is restored.[16] This modulates the complex dielectric function of the sample, and thus the refractive index, which in turn leads to the measured fractional change in reflectivity $\Delta R/R$.

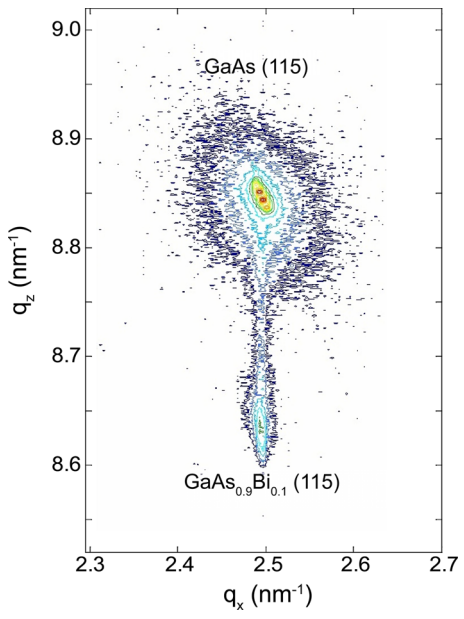

FIG. 1. XRD reciprocal space map of a $GaBi_xAs_{1-x}$ film on GaAs substrate with $x = 10.4\%$, for the (115) XRD reflection. The horizontal scale is the in-plane reciprocal space q vector, and the vertical the out-of-plane q. The upper cluster of points corresponds to the XRD peak from the GaAs substrate while the lower peak is due to the GaBiAs film, with the intensity indicated by colour (red being the most intense, black the least). Since the film and substrate have the same in-plane q (and thus the same in-plane lattice constant), the film is pseudomorphic to the GaAs substrate, to within the measurement error ($<\pm 2\%$).

II. EXPERIMENT

The interband transition energies between the CB and HH^+/LH^+ VB edges (E_g^{HH+} and E_g^{LH+}), and between the CB and SO^+ band edges (E_g^{SO+}), were measured at room temperature. A 514 nm argon-ion laser line chopped at a frequency of 333 Hz, of power 126 mW, was used to modulate the same spot on the sample as illuminated by the probe beam from a tungsten filament lamp and single-grating monochromator. Phase sensitive detection of the PR signal was performed with a lock-in amplifier connected to either InGaAs or Si PIN photodiodes, depending on the wavelength region being studied. The measured PR spectral line shapes were least-squares fitted using the sum of two Aspnes third derivative functional forms (TDFFs) (Ref. 17)

$$\Delta R/R = Re[Ce^{i\theta}(E - E_g + i\Gamma)^{-n}], \quad (1)$$

where C and θ are amplitude and phase variables, E the energy of the probe beam, E_g the critical point transition energy, and Γ a broadening parameter. We investigated the effect of choosing several of the suggested values for the line shape exponent factor n (Ref. 17) but found that this had little influence on the fitted transition energies. Here, we present the results for fits using $n = 3$.

Figure 2(a) shows the resulting room temperature PR spectra for the four $GaBi_xAs_{1-x}$ ($2.3\% \leq x \leq 10.4\%$) samples in the region of the fundamental bandgap of GaBiAs. The two low-energy composition-dependent features correspond to the CB-HH^+ and CB-LH^+ transitions in $GaBi_xAs_{1-x}$, and the curves show their fits with two TDFFs. The composition-independent highest-energy transition near 1.43 eV is related to the GaAs bandgap of the cap/substrate. It may be noted from Fig. 2(a) that the fit with two TDFFs for the highest bismuth concentration of 10.4% is rather poor in the energy region between the HH^+ and LH^+ features. This may be an indication of the predicted emergent effects of stronger LH interactions with Bi-Bi and Bi cluster states, with increasing strain and bismuth content.[18]

Figure 2(b) shows the measured PR features in the region of the spin-orbit split-off transition, showing the composition-dependent CB-SO^+ transition for the $GaBi_xAs_{1-x}$ as well as the corresponding composition-independent SO transition for GaAs.

In Fig. 2(a), we observe a significant composition-dependent red-shift in the HH^+ bandgap energy E_g^{HH+} with the increasing bismuth concentration. For the 10.4% sample, a HH^+ bandgap wavelength of 1.52 μm has been achieved at room temperature. In Fig. 2(b), the effect of bismuth concentration of up to 10.4% on the SO^+ transition can be seen. Figure 3 shows the three fitted PR transition energies: E_g^{SO+}, E_g^{HH+}, and E_g^{LH+}. Such a composition dependence of the interband transitions has been attributed to the band anti-crossing interaction of the Bi level with the VB of GaAs.[3]

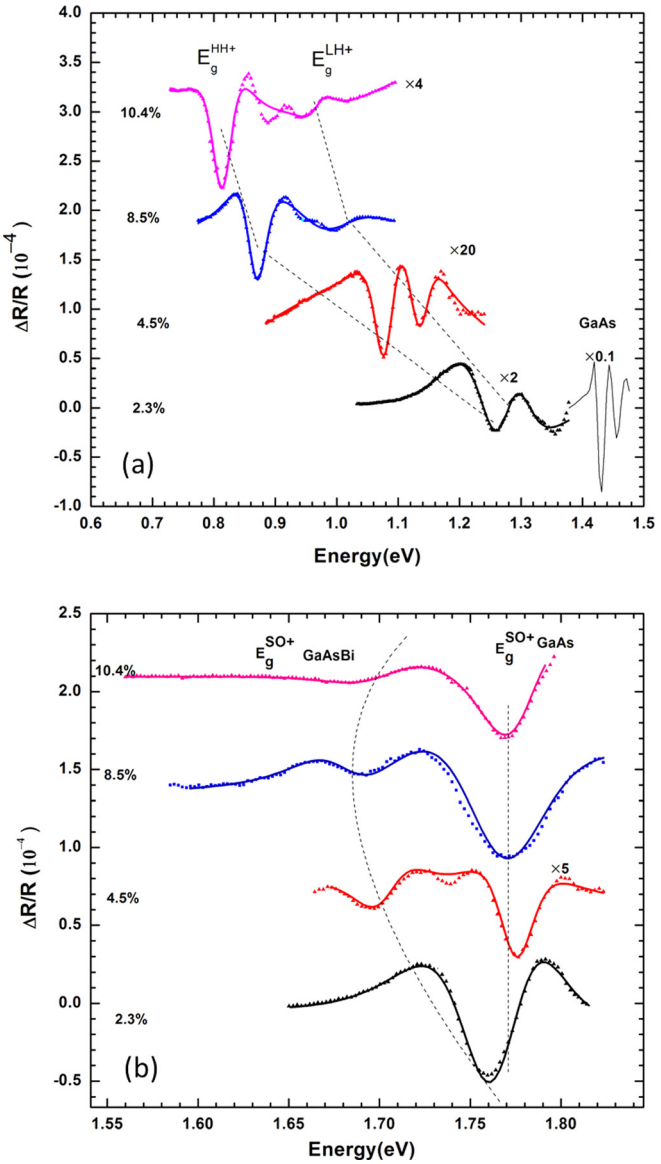

FIG. 2. (a) Room temperature PR spectra for the four compressively strained $GaBi_xAs_{1-x}$ samples studied here, in the region of the fundamental bandgap. Circles are the experimental data points and solid curves are fits with a sum of two TDFFs—one each for the HH^+ and LH^+ features, where these refer to heavy-(HH^+) and light-hole (LH^+) transitions, respectively. The feature to the far right is due to the GaAs cap/substrate and does not vary with bismuth content. The dashed lines are guides to the eye of the approximate positions of the fitted transition energies. (b) Room temperature PR spectra for the four compressively strained $GaBi_xAs_{1-x}$ samples studied here, in the region of the spin-orbit split off transition. Circles are the experimental data points and solid curves are fits with a sum of two TDFFs—one for the $GaBi_xAs_{1-x}$ feature and another for the GaAs feature. The dashed curves are guides to the eye of the approximate positions of the fitted transition energies.

The E_g^{HH+} and E_g^{LH+} PR features in Fig. 2(a) are due to the strain-induced VB splitting in this alloy due to the lattice mismatch to GaAs. Figure 4 shows that the VB splitting ($VBS = E_g^{LH+} - E_g^{HH+}$) changes approximately linearly with bismuth content, at a rate of 15.0 ± 1 meV/%Bi, which is in good agreement with the 15.1 meV/%Bi reported by Francoeur *et al.*[2] The error bars in Fig. 4 represent the combined uncertainties in the VBS from the associated errors in the fitted transition energies taken from the least-squares program correlation matrix.

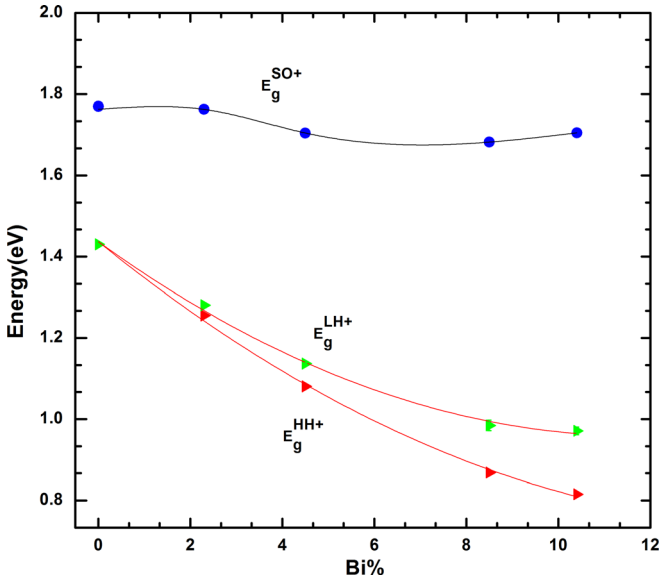

FIG. 3. Transition energy values E_g^{HH+}, E_g^{LH+}, and E_g^{SO+} obtained by fitting the room temperature experimental PR spectra of Figs. 2(a) and 2(b) with TDFFs. The curves are only guides to the eye. The fitting uncertainties are within the symbol size.

By using the results of Fig. 3, we can plot the splittings $E_g^{SO+} - E_g^{HH+}$ and $E_g^{SO+} - E_g^{LH+}$, which are equivalent to the transition energy values from the SO^+ to HH^+ and LH^+ valence band edges, respectively. Figure 5 shows that $E_g^{SO+} - E_g^{HH+}$, the splitting between the SO^+ and the top of valence band (which is heavy hole in this case) becomes equal to the observed HH^+ transition energy E_g^{HH+} at a bismuth concentration of $\sim 9.0 \pm 0.2\%$ in these strained samples. This result has importance for device applications due to the possibility of reducing the CHSH Auger losses involving hole excitation into the spin-orbit band at higher bismuth concentrations.

By using all our experimental values for these strained samples, we calculate the deformation potential (b) next and, by decoupling the effects of strain in our samples, the

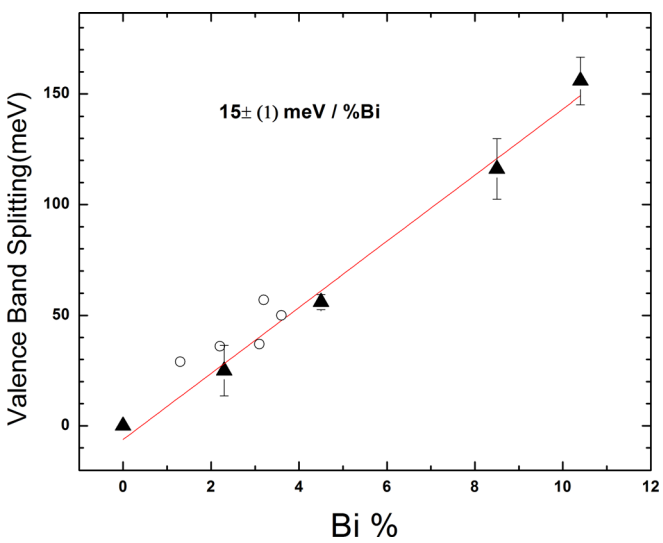

FIG. 4. VB splitting ($VBS = E_g^{LH+} - E_g^{HH+}$) as a function of bismuth concentration in our compressively strained $GaBi_xAs_{1-x}$ samples. The open circles are the corresponding results of Francoeur *et al.*[2]

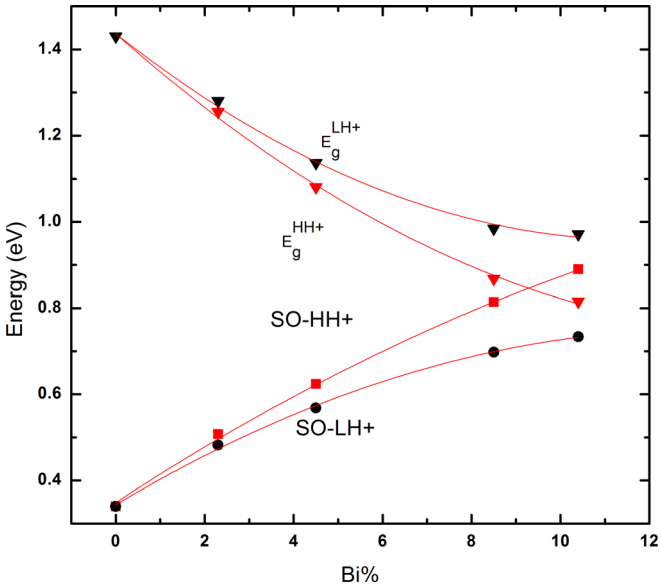

FIG. 5. Fitted transition energy values E_g^{HH+}, E_g^{LH+} and the differences between these and the E_g^{SO+} results in Fig. 3, as a function of bismuth concentration. Fitting uncertainties are within the symbol size.

bandgap (E_{go}) and the spin orbit splitting energy (Δ_o) for free standing GaBiAs material.

III. THEORY, ANALYSIS, AND DISCUSSION

The in-plane biaxial strain along the x and y directions is defined by

$$\varepsilon_{xx} = \varepsilon_{yy} = \frac{(a_{GaAs} - a_{GaBiAs})}{a_{GaBiAs}}, \tag{2}$$

where a_{GaBiAs} is the lattice constant of GaBiAs, which we calculate using Vegard's law; $a_{GaBi_xAs_{1-x}} = (1-x)\, a_{GaAs} + x a_{GaBi}$.

As GaBi has not yet been grown, there is no experimental value of its lattice constant. We therefore used its theoretically calculated value, $a_{GaBi} = 6.324$ Å,[19] and the accepted value for GaAs, $a_{GaAs} = 5.653$ Å.[20] The out-of-plane strain along the growth z-direction is defined by

$$\varepsilon_{zz} = -\left(\frac{2c_{12}}{c_{11}}\right)\varepsilon_{xx}, \tag{3}$$

where c_{11} and c_{12} are the elastic constants of $GaBi_xAs_{1-x}$. As the elastic constants for $GaBi_XAs_{1-x}$ and GaBi are again not known, we used the $c_{11} = 12.21$ and $c_{12} = 5.66$ (units of 10^{11} dyn/cm^2) values for GaAs.[20] Since we require only the ratio $2c_{12}/c_{11}$, which is approximately unity for all III-V semiconductors, the use of the GaAs values is justifiable for all the bismuth concentrations studied here. The resulting in-plane and out-of-plane strain components calculated for our $GaBi_xAs_{1-x}$ epilayers are shown in Fig. 6.

The strain-induced HH^+-LH^+ VB splitting in Fig. 4 may be used to calculate the shear deformation potential for this material. Conventionally, the effects of strain can be modelled within the 8-band strain-dependent k.p perturbation treatment.[21] Here, we will assume this can also be

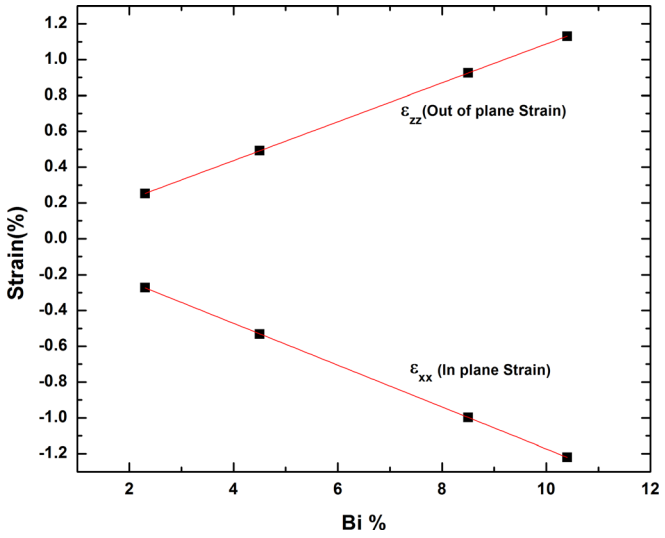

FIG. 6. In-plane and out-of-plane strain vs. bismuth concentration in the $GaBi_xAs_{1-x}$ layers.

applied to the E^+ band structure of this more complex alloy. However, since we are interested in the fundamental and spin-orbit splitting bandgaps at the centre of the Brillouin zone (i.e., $k = 0$), the coupling between the CB and VBs disappears in the 8-band strain Hamiltonian, reducing it to the corresponding 6-band form.[22] Upon diagonalisation, this yields the well-known expressions for the strain dependent heavy-hole, light-hole, and spin-split-off bandgaps at $k = 0$, such as those given in Ref. 23. Hence, as in the case of the band anti-crossing system dilute-N GaAsN,[24] the following equations may be used for the strained HH^+, LH^+, and SO^+ transition energies:

$$E_g^{HH+} = (E_{go} + \delta E_H) + \delta E_s, \tag{4}$$

$$E_g^{LH+} = (E_{go} + \delta E_H) + \frac{1}{2}(\Delta_o - \delta E_S) - Q, \tag{5}$$

$$E_g^{SO+} = (E_{go} + \delta E_H) + \frac{1}{2}(\Delta_o - \delta E_S) + Q, \tag{6}$$

where E_{go} is the unstrained fundamental bandgap energy (between the CB and degenerate HH^+/LH^+ edges) and Δ_o is the spin-orbit splitting energy (between the SO^+ and degenerate HH^+/LH^+ edges). The other quantities are defined as

$$Q = \frac{1}{2}\sqrt{(\Delta_o^2 + 2\Delta_o \delta E_s + 9\delta E_S^2)},$$

$$\delta E_s = b(\varepsilon_{zz} - \varepsilon_{xx}), \text{ and}$$

$$\delta E_H = a(2\varepsilon_{xx} + \varepsilon_{zz}).$$

Here b is the shear deformation potential and $a = a_c + a_v$ the hydrostatic deformation potential. a_c and a_v are the CB and VB hydrostatic deformation potentials, respectively. For our analysis, we use the values $a_c = -7.17$ eV and $a_v = -1.16$ eV from GaAs.[20] These values are not very different from those of GaSb (which is expected to be more similar to GaBi than GaAs); the sum $(a_c + a_v)$ that is used in the calculations is almost the same for GaBi and GaSb.

If we define the VBS as $\Delta_{LH} = E_g^{LH+} - E_g^{HH+}$, then from Eqs. (4) and (5) we have

$$\Delta_{LH} = \frac{1}{2}\Delta_0 - \frac{3}{2}\delta E_s - Q. \tag{7}$$

If, as suggested by Zhang *et al.*,[24] we were to assume that $\Delta_0 \gg |b(\varepsilon_{zz} - \varepsilon_{xx})|$ in the expression for Q, then using Eq. (7) we can derive the following approximate expression for the shear deformation potential:

$$b \approx \frac{-\Delta_{LH}}{2(\varepsilon_{zz} - \varepsilon_{xx})}. \tag{8}$$

However, this approximation is not necessary here because we have the additional information needed in Eq. (7) from our measurements of E_g^{SO+}. From Eq. (7), we obtain

$$\Delta_o^2 + 2\Delta_o\delta E_s + 9\delta E_S^2 = [(\Delta_0 - 2\Delta_{LH}) - 3\delta E_s]^2,$$

from which we get

$$\delta E_s = \frac{-\Delta_{LH}}{\left(2 + \frac{1}{1-\frac{\Delta_o}{\Delta_{LH}}}\right)}. \tag{9}$$

From the definition of

$$\delta E_s = b(\varepsilon_{zz} - \varepsilon_{xx}),$$

we then have

$$b = \frac{1}{(\varepsilon_{zz} - \varepsilon_{xx})} \times \frac{-\Delta_{LH}}{\left(2 + \frac{1}{1-\frac{\Delta_o}{\Delta_{LH}}}\right)}. \tag{10}$$

Note that Eq. (10) reduces to Eq. (8) if $\Delta_o \gg \Delta_{LH}$.

In order to use Eq. (10) to obtain b, we require the values of spin orbit splitting (Δ_o). The theory of Eqs. (4)–(6) allows us to deduce Δ_o from our experimental measurements, by the following method. Subtracting Eqs. (5) and (6), we obtain a quantity $\Delta_{SO/LH} = E_g^{SO+} - E_g^{LH+} = 2Q$. Squaring this and re-arranging, we obtain a quadratic in Δ_o with the solutions

$$\Delta_0 = -\delta E_S \pm \sqrt{(\Delta_{SO/LH}^2 - 8\delta E_S{}^2)}. \tag{11}$$

This, together with Eq. (9), may be solved for Δ_o by the following iteration scheme:

1. Make an initial guess for Δ_o from, say, the bigger of $E_g^{SO+} - E_g^{LH+}$ and $E_g^{SO+} - E_g^{HH+}$ (as in Fig. 5).
2. Use this estimate of Δ_o and our experimental value of Δ_{LH} to estimate δE_s from Eq. (9).
3. Use this δE_s and our experimentally measured $\Delta_{SO/LH}$ to obtain the next estimate of Δ_o from Eq. (11).
4. Repeat steps 2 and 3 until convergence occurs for the Δ_o value.

Substituting the resulting deduced Δ_o and the values for Δ_{LH}, ε_{zz} and ε_{xx} for $GaBi_xAs_{1-x}$ into Eq. (10) then gives the shear deformation potential for the different concentrations of bismuth. We first consider these results for b, as shown in Fig. 7, and discuss the Δ_o results later.

The error bars in Fig. 7 come from considering mainly the errors in the VBS in Eq. (10), as shown in Fig. 4. Thus, the calculated error bar for b is largest in the 2.3% sample, due to the close proximity of the HH^+ and LH^+ features in the PR spectra, and the consequently proportionally higher fitting errors in the VBS. Figure 7 shows that the deformation potential for compressively strained GaBiAs layers is composition dependent, as has been found for the dilute-N GaAsN alloys.[24] Due to the big difference in the size of the bismuth atom, as compared to the arsenic atom it replaces, a shear strain field is induced in its vicinity, which is responsible for the perturbations in the VBS and deformation potential.[25] In the case of N in GaAs, Zhang *et al.*[24] argue that as the nitrogen content increases, these local strain fields interact and lead to an overall additional strain, which will in turn lead to an increase in the VBS. The GaAsN b has an even more complex composition dependence on N content[24] than in our case of GaBiAs, which appears approximately linearly dependent on bismuth content up to 10.4% (see Fig. 7). The reason for this dependence is not understood for this new alloy at present.

Once Δ_o and b have been deduced by the above methods, we can then use Eq. (4), say, to deduce the unstrained bandgap energy for free-standing GaBiAs, $E_{go} = E_g^{HH+} - (\delta E_H + \delta E_s)$, from our measurement of E_g^{HH+} (Fig. 3), the known values of a and b (from Fig. 7), and the calculated strains ε_{xx} and ε_{zz} (from Fig. 6).

The resulting deduced spin-orbit splitting energy and unstrained bandgap energy are shown in Fig. 8 (filled triangles). We estimate from a small extrapolation of the curves in Fig. 8 that the energy cross-over $\Delta_o = E_{go}$ would occur at bismuth concentrations of $10.5 \pm 0.2\%$ for such free-standing GaBiAs.

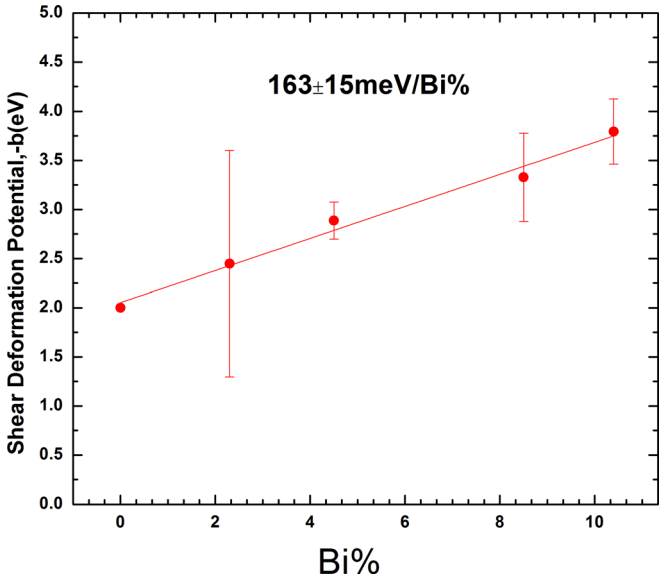

FIG. 7. Deduced shear deformation potential of coherently compressively strained $GaBi_xAs_{1-x}$ on a GaAs substrate as a function of bismuth concentration. The linear fit gives a gradient of 163 meV/%Bi.

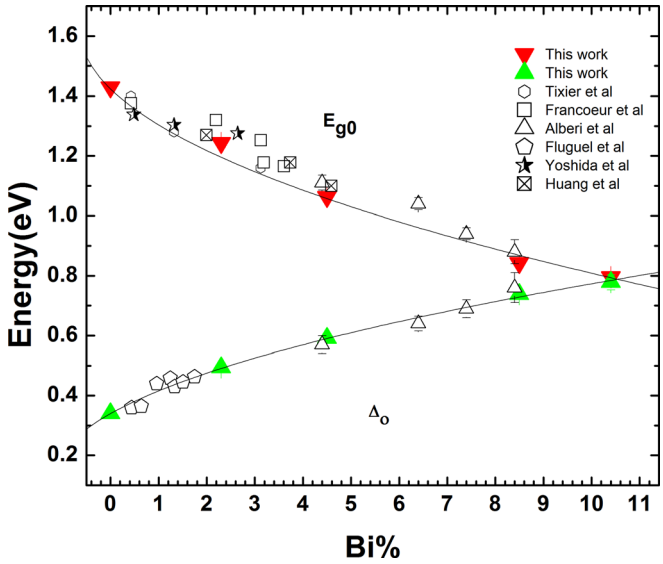

FIG. 8. The filled triangles show the composition-dependence of the room temperature spin-orbit splitting energy Δ_o and unstrained bandgap energy E_{go} for free-standing GaBiAs as deduced from our experimental measurements. The curves are guides to the eye through our results. The other symbols show the results of other authors.[1–3,5,9,26] Our results extend the previous work to 10.4% bismuth and predict that $\Delta_o = E_{go}$ at $10.5 \pm 0.2\%$ bismuth for the unstrained free-standing material.

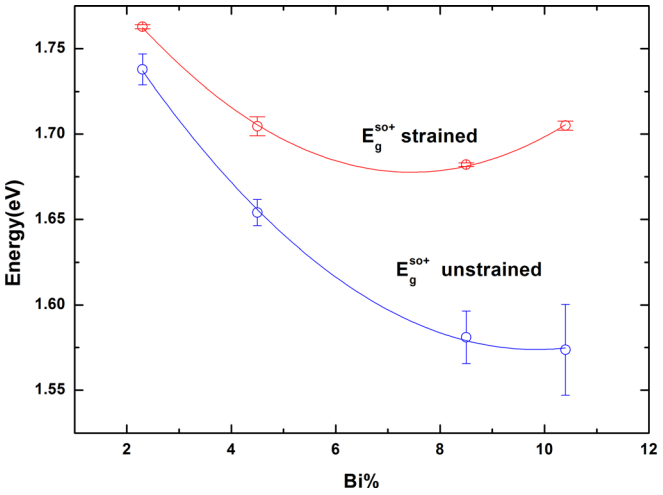

FIG. 9. The upper plot shows our room temperature measurements of the spin-orbit split-off transition energy in compressively strained GaBiAs, as a function of bismuth concentration, compared to our predictions of the same transition in free-standing GaBiAs (lower plot). The curves are guides to the eye.

Figure 8 also compares our results for Δ_o and E_{go} with the values of other authors, for which the GaBiAs materials are reported, or assumed by those authors, to be for relaxed unstrained GaBiAs (except those of Francouer *et al.*[2]). Clearly there is a satisfactory agreement with many of the other results. Our results extend the previous work to 10.4% bismuth concentration and provide a clear indication of the expected cross-over composition for free-standing GaBiAs. We might remark in passing that the fundamental bandgap PR spectra of the ~4% and ~7% Bi samples of Ref. 3 seem to show a HH/LH splitting, similar to that observed here and which we attribute to strain. However, those authors do not comment on their observation.

It is also of interest to deduce where the SO^+ split-off transition energy E_g^{SO+} $(=E_{go}+\Delta_o)$ would lie in the free-standing equivalent of our samples. The data required for this calculation are in Fig. 8 and the results are shown in Fig. 9, together with the direct measurements of E_g^{SO+} in our strained samples. This deduced behaviour of E_g^{SO+} in the unstrained material shows a considerable red-shift in the CB-SO transition energy with bismuth content, which is entirely due to the VB anti-crossing effect. Now in our samples, compressive strain acts to push the SO^+ band down in energy, while pushing the CB up. This contributes a blue-shift to E_g^{SO+}, which increases with bismuth fraction, and is opposite to the red-shift for the unstrained E_g^{SO+}. As is evident from Fig. 9, this strain-induced blue-shift eventually overcomes the anti-crossing-induced red-shift in the unstrained E_g^{SO+}, at the highest bismuth fraction in our samples. It has been predicted that the inclusion of bismuth has only a relatively weak red-shift effect on the energy of the unstrained SO^+ band edge.[3] Therefore, the observation in Fig. 9 of a significant decrease in the unstrained E_g^{SO+} (~21 meV/%Bi) indicates that the CB edge must also be moving down in energy with increasing Bi content. Since the bandgap of GaBiAs is smaller than that of GaAs, and the CB edge is lower, then the VB edge must be above that of GaAs. Thus, a type-I conduction/valence band alignment is expected for dilute-Bi GaBiAs on GaAs. These conclusions are consistent with very recent theoretical tight binding studies of the band structure of free-standing bulk GaBiAs which predict that the CB edge drops about five times faster than the SO edge with bismuth concentration, giving a net red-shift in the CB-SO transition energy of ~22 meV/%Bi.[18]

IV. SUMMARY AND CONCLUSIONS

In summary, the electronic band structure of the bismide alloy $GaBi_xAs_{1-x}$ in the energy regions of both the fundamental bandgap and spin orbit split off feature has been studied as a function of bismuth concentration. Room temperature photoreflectance measurements on compressively strained $GaBi_xAs_{1-x}$ layers on GaAs substrates, with Bi concentrations between 2.3% and 10.4%, show that the energy of the strained heavy-hole bandgap E_g^{HH+} is resonant with the difference in energy between the HH^+ and SO^+ band edges at a bismuth concentration of $\sim 9.0 \pm 0.2\%$. We also determine that the strain-induced valence band (HH^+-LH^+) splitting increases with bismuth concentration at a rate of $\sim 15 \pm 1$ meV/%Bi. From this we calculate the shear deformation potential b of these compressively strained GaBiAs layers and find that this increases in magnitude with bismuth content at a rate of $\sim 163 \pm 15$ meV/%Bi. Finally, we have used iterative strain theory calculations to decouple the effects of strain in our experimental measurements and thus estimate the spin-orbit splitting energy Δ_o and the bandgap E_{go} of free-standing GaBiAs: we find that these are in resonance, $\Delta_o = E_{go}$, at a bismuth concentration of $\sim 10.5 \pm 0.2\%$. Furthermore, our study suggests that the band alignment for GaBiAs grown on GaAs will be type-I, in line with recent theoretical predictions.

ACKNOWLEDGMENTS

Z.B. gratefully acknowledges the support of the "The Islamia University of Bahawalpur, Pakistan" for providing a studentship under the Faculty Development Program (FDP) and also further partial support from the "Surrey Kwan Trust Fund." This work was also partially funded by the EPSRC under EP/G064725/1. T.J.C.H. thanks the "Malaysian University Grant Program (GUP) Tier 1," Universiti Teknologi Malaysia and M.O.H.E. (Q.J130000.7126.01H55). We are grateful to Vahid Bahrami Yekta and Mostafa Masnadi of the University of Victoria, Canada, for providing the XRD measurements of Fig. 1.

[1]S. Tixier, M. Adamcyk, T. Tiedje, S. Franceour, A. Mascarenhas, P. Wei, and F. Schiettekatte, Appl. Phys. Lett. **82**, 2245 (2003).
[2]S. Francoeur, M. J. Seong, A. Mascarenhas, S. Tixier, M. Adamcyk, and T. Tiedje, Appl. Phys. Lett. **82**, 3874 (2003).
[3]K. Alberi, O. D. Dubon, W. Walukiewicz, K. M. Yu, K. Bertulis, and A. Krotkus, Appl. Phys. Lett. **91**, 051909 (2007).
[4]Y. Zhang, A. Mascarenhas, and L. W. Wang, Phys. Rev. B **71**, 155201 (2005).
[5]B. Fluegel, S. Francoeur, A. Mascarenhas, S. Tixier, E. C. Young, and T. Tiedje, Phys. Rev. Lett. **97**, 067205 (2006).
[6]J. P. Loehr and J. Singh, IEEE J. Quantum Electron. **29**, 2583 (1993).
[7]S. J. Sweeney, Photonics West 2010, Paper [7616-11] (2010).
[8]S. J. Sweeney, WO patent 2010/149978 (2010).
[9]J. Yoshida, T. Kita, O. Wada, and K. Oe, Jpn. J. Appl. Phys. **42**, 371 (2003).
[10]K. Oe, Jpn. J. Appl.Phys. **41**, 2801 (2002).
[11]G. Pettinari, A. Polimeni, M. Capizzi, J. H. Blokland, P. C. M. Christianen, J. C. Maan, E. C. Young, and T. Tiedje, Appl. Phys. Lett. **92**, 262105 (2008).
[12]D. G. Cooke, F. A. Hegmann, E. C. Young, and T. Tiedje, Appl. Phys.Lett. **89**, 122103 (2006).
[13]V. Pacebutas, K. Bertulis, G. Aleksejenko, and A. Krotkus, J. Mater. Sci: Mater. Electron. **20**, S363 (2008).
[14]X. Lu, D. A. Beaton, R. B. Lewis, T. Tiedje, and Y. Zhang, Appl. Phys. Lett. **95**, 041903 (2009); X. Lu, D. A. Beaton, R. B. Lewis, T. Tiedje, and M. B. Whitwick, *ibid.* **92**, 192110 (2008).
[15]F. H. Pollak, *Handbook on Semiconductors*, edited by T. S. Moss (Elsevier, Amsterdam, 1994), Vol. 2, p. 527.
[16]H. Shen, Z. Hang, S. H. Pan, F. H. Pollak, and J. M. Woodall, Appl. Phys. Lett. **52**, 2058 (1988).
[17]D. E. Aspnes, Surf. Sci. **37**, 418 (1973).
[18]M. Usman, C. A. Broderick, A. Lindsay, and E. P. O'Reilly, Phys. Rev. B **84**, 245202 (2011).
[19]A. Janotti, S.-H. Wei, and S. B. Zhang, Phys. Rev. B. **65**, 115203 (2003).
[20]I. Vurgaftman, J. R. Meyer, and L. R. Ram-Mohan, J. Appl.Phys. **89**, 5825 (2001).
[21]T. B. Bahder, Phys. Rev. B **41**, 11992 (1990).
[22]C. Pryor, Phys. Rev. B **57**, 7190 (1998).
[23]F. H. Pollak, *Semiconductors and Semimetals*, edited by T. P. Pearsall (Academic, New York, 1990), Vol. 32, p. 17.
[24]Y. Zhang, A. Mascarenhas, H. P. Xin, and C. W. Tu, Phys. Rev. B **61**, 4433 (2000).
[25]T. N. Morgan, in *Proceedings of the 10th International Conference on the Physics of Semiconductors*, August 17–21, 1970, p. 266.
[26]W. Huang, K. Oe, G. Feng, and M. Yoshimoto, J. Appl. Phys. **98**, 053505 (2005).